Dean&Francis
ISSN 2959-409X

Research on Wearable Electrochemical Sensors for Sweat Analysis

Linlin Ren[1, *]

[1]School of Information and Communication Engineering, Communication University of China, Beijing, China
*Corresponding author: 202311043002@mails.cuc.edu.cn

Abstract:

There has long been a significant gap between cutting-edge research and practical product application in the field of wearable sweat sensors. This paper reviews two seminal publications (2017, 2020) in the domain of wearable sweat sensing. The research content primarily focuses on two aspects: the system integration capability based on commercial modules, as explored in the 2017 study "Research on a Real-time Detection System for Wearable Sweat Composition", and the investigation into high-performance flexible fibers and novel materials, as presented in the 2020 study "Solid-state Ion-selective Analysis for Wearable Sweat Monitoring". This article provides a focused analysis of the technological pathways adopted by these two studies and their subsequent influence on the field. The 2017 work accelerated the translation of laboratory prototypes toward commercialization, while the 2020 study opened new possibilities for long-term, comfortable monitoring through material innovation. Together, they represent two distinct yet complementary approaches to advancing wearable sweat sensing from concept to reality.

Keywords: Wearable sweat sensors, Electrochemical sensing, Real-time monitoring.

1. Introduction

With the integration of flexible electronics and biosensing technologies, wearable sweat sensors have attracted significant attention from both academia and industry in recent years as crucial tools for personalized health monitoring. Sweat contains a variety of biomarkers and is closely associated with physiological states, which offers the potential for non-invasive and continuous bodily fluid analysis. However, the development of this field exhibits a distinct dichotomy: on one hand, fundamental research continues to make breakthroughs in material innovation and sensing mechanisms; on the other, there remains a scarcity of mature solutions that can achieve practical and commercial application.

As early as 2017 to 2020, the technological pathways in wearable sweat sensing had begun to take shape. The 2017 study "Research on a Real-Time Detection System for Wearable Sweat Composition" pioneered a system integration approach based on commercial modules[1], demonstrating the feasibility of rapidly

constructing wearable sensing systems. The 2020 paper "Solid-State Ion-Selective Analysis for Wearable Sweat Monitoring" represented a material-driven strategy, achieving notable progress in flexible fibers and sensitive materials[2]. Although these early studies illustrated the technical feasibility from different perspectives, wearable sweat sensors have yet to achieve large-scale adoption years later, with industrialization lagging significantly behind technological development.

This challenge stems not from technical infeasibility, but rather from structural barriers commonly encountered in the transformation of scientific and technological achievements. Non-technical factors such as cost control, engineering implementation, system integration, and market positioning collectively form a substantial gap between laboratory research and market application. Even subsequent studies, like "Real-Time Sensing Characteristics of Flexible Sweat Sensors Based on Microfluidic Systems", still remains to focus on improving sensors, while more effort is needed before practical deployment [3].

To systematically examine the underlying reasons for this phenomenon, this paper selects the aforementioned representative early literature and reviews the development trajectory of wearable sweat sensors from a historical perspective. By comparing the characteristics and limitations of different technological pathways, it aims to reveal key bottlenecks in the technology translation process and provide valuable reflections and insights for the field's future development.

2. Organization of the Fundamentals of Sweat Sensing and System Integration

2.1 Overview of Sweat Biomarkers

Among various bodily fluids used for detection, sweat has not yet received widespread attention as a biological sample; however, its potential is considerable [4]. Primarily secreted by sweat glands in the skin, sweat is a clean, hypotonic fluid composed mainly of water, along with various electrolytes and small organic molecules. Additionally, trace metal ions, proteins, peptides, inhibitors, antibodies, antigens, and certain exogenous substances such as drugs and ethanol can also be detected in sweat [5]. During the process of sweat secretion from glands to the skin surface, reabsorption of electrolytes such as sodium and chloride ions occurs. Certain diseases can alter the concentration of sweat components or lead to the emergence of new constituents, highlighting the potential of sweat as a source of biomarkers for related conditions [6].

The early clinical application of sweat focused on the diagnosis of cystic fibrosis. This disease, caused by mutations in the gene encoding the cystic fibrosis transmembrane conductance regulator, disrupts the transport of chloride and sodium ions in epithelial cells, leading to dysfunction in the lungs, pancreas, and liver [7]. Measuring sodium and chloride ion concentrations in sweat can effectively aid in diagnosing cystic fibrosis [8]. Furthermore, sweat is suitable for drug monitoring. During the absorption, breakdown, and metabolism of drugs in the body, some metabolites are excreted through sweat [9]. Compared to urine samples, sweat is less susceptible to adulteration, and studies indicate that the detection window for certain drugs in sweat may be longer than in urine, making sweat a viable medium for long-term, continuous monitoring of drug abuse [10]. Certain heavy metal ions (e.g., lead, mercury, arsenic) absorbed through the skin are also primarily excreted via sweat. Their detection in sweat occurs earlier than in blood or urine, and the excretion volume is more significant [11]. Common electrolytes such as sodium, potassium, and magnesium ions are also easily detectable in sweat.

Beyond these applications, sweat can be used for alcohol detection, as well as genomics and proteomics research [12]. The pH of sweat is also an important indicator of health status. M. H. Schmid-Wendtner et al. noted that the mechanisms of certain skin diseases, such as irritant/contact dermatitis and acne, are associated with changes in skin surface pH [13]. Patterson et al. found that when metabolic alkalosis was induced by sodium bicarbonate intake, the pH of both blood and sweat increased [14]. Other studies have shown a correlation between pH and sodium ion concentration in isolated sweat glands [15]. Continuous monitoring of sweat pH during exercise can help provide early warnings of alkalosis risks. By enabling scientific hydration and nutritional interventions, it can also enhance athletic performance, which underscores the importance of real-time sweat pH monitoring.

2.2 Principles of Electrochemical Sensing

The pH sensor used in this system employs an antimony electrode as the indicator electrode and an Ag-AgCl electrode as the reference electrode. The antimony electrode belongs to the metal–metal oxide electrode system and is made of spectroscopically pure antimony. The formation of its electrode potential originates from the interfacial reaction between the metal and its surface oxide layer. When the antimony electrode comes into contact with the solution being measured, its surface is oxidized, forming a thin film of Sb_2O_3. The potential difference between the metallic antimony and the oxide layer depends on the

ISSN 2959-409X

concentration of Sb_2O_3, which is closely related to the hydrogen ion concentration in the solution. Therefore, the pH value of the solution can be reflected by measuring the potential difference between antimony and antimony trioxide. The corresponding chemical reactions are as follows:

$$2Sb + 3H_2O \longleftrightarrow Sb_2O_3 + 6H^+ \quad (1)$$

$$Sb_2O_3 + 6H^+ \longleftrightarrow 2Sb^{+3} + 3H_2O \quad (2)$$

This sensor operates based on the quantitative relationship between the indicator electrode and the activity of H^+ions in the solution. Using the Ag-AgCl electrode as the reference electrode, it forms a closed measurement circuit with the antimony electrode to measure the acidity or alkalinity of the solution. When the hydrogen ion concentration in the solution changes, the output potential E of the indicator electrode varies accordingly, following the Nernst equation:

$$E = E_0 - \frac{2.303RT}{nF} pH \quad (3)$$

$$E - E_0 = -k \times pH \quad (4)$$

where E is the output potential of the sensing element, E_0 is the standard potential of the sensing element, R is the ideal gas constant, T is the thermodynamic temperature, n is the charge number of the ion involved in the reaction, and F is the Faraday constant.

It can be concluded that the output potential of the sensing element exhibits a linear relationship with the pH of the solution, where the slope k is a function of temperature T, expressed as:

$$k = \frac{2.303RT}{nF} = 54.157 + 0.1984t \quad (5)$$

In this system, the effect of temperature is negligible due to its minimal variation, and k is considered constant. Before measurement, the values of $E_0$and k can be calibrated using a standard pH meter.

2.3 Basic Components of Wearable Systems

The hardware of the system primarily consists of a sensor module, a signal processing circuit, a central microprocessor, a wireless communication module, and a power management unit.

The sensor module employs an antimony electrode as the measuring electrode and an Ag-AgCl electrode as the reference electrode. pH detection is achieved by measuring the electrode potential difference between antimony and its surface antimony trioxide (Sb_2O_3,). For temperature measurement, an LM35 temperature sensor is used, which provides an output voltage linearly proportional to the Celsius temperature.

The signal processing circuit includes amplification and filtering stages. The output from the pH sensor is a millivolt-level weak signal, which requires amplification for conditioning. In contrast, the output from the temperature sensor is at the volt level and can be processed directly. To enhance anti-interference capability, a high-frequency filter module is incorporated into the circuit design to suppress environmental high-frequency noise and 50 Hz power-line interference.

The central microprocessor is an Arduino R3 development board, with software developed using the Arduino IDE. Its main functions include sensor signal acquisition, analog-to-digital (A/D) conversion, data processing, result display, and communication control with the Bluetooth module.

Wireless transmission is handled by an HC05 master-slave integrated Bluetooth serial module, which transmits the processed data from the microprocessor to a mobile terminal. The mobile application is developed using Android Studio and written in Java, enabling Bluetooth communication and real-time reception and display of measurement data.

The power supply unit uses three 3V button cells connected in series, primarily providing operating voltage to the microprocessor. The signal processing circuit and the Bluetooth module are powered by the onboard power supply of the microprocessor board.

3. Case Studies: From Technological Breakthroughs to System Integration

3.1 A Fully Integrated Wearable System with pH Sensing and Wireless Transmission

After uploading the program to the Arduino Uno, the system is assembled as shown in Fig.1. The Arduino Uno is connected to the LCD display and the HC-05 Bluetooth serial module. The LM35 temperature sensor is connected to analog input pin A4, while the pH sensor, after passing through the signal processing circuit, is connected to analog input pin A4. A 9V button battery is used to power both the signal processing circuit and the Arduino Uno. Fig.2 shows the physical assembly.

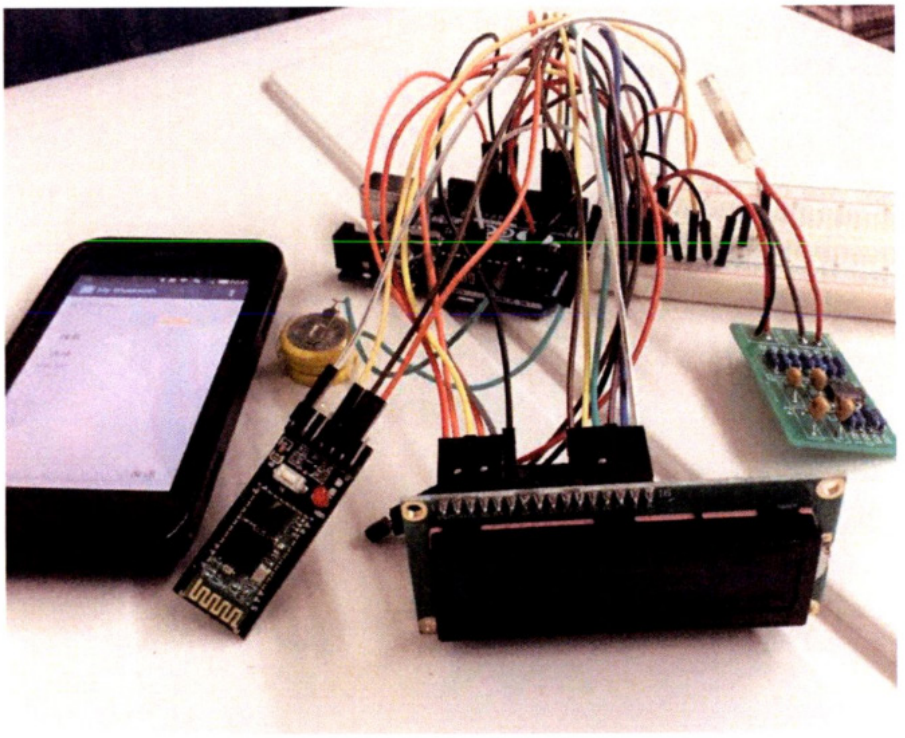

Fig. 1 System Overall Debugging Diagram

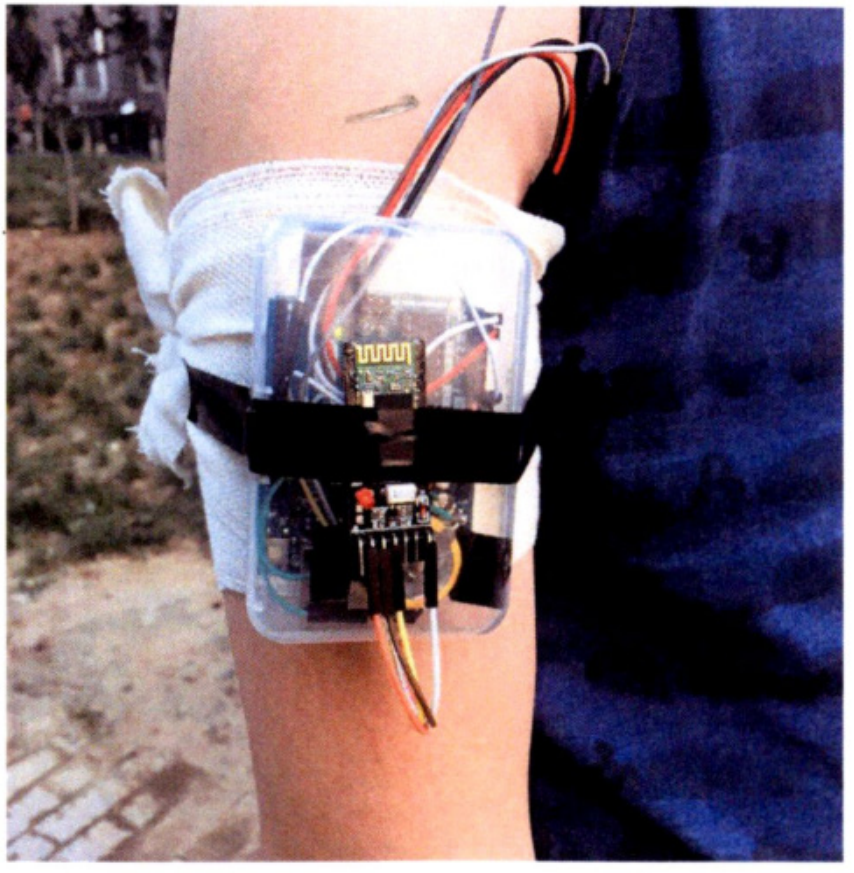

Fig. 2 Volunteer Wearing the Sweat Detection Device

ISSN 2959-409X

A line chart was plotted based on the measured sweat pH variation data, as shown in Fig.3. The graph indicates that the sweat pH value increased continuously during the initial stage, with the rate of increase slowing down after 8 minutes. A declining trend was observed after 16 minutes, followed by a renewed upward trend after 28 minutes.

Analysis of these changes suggests that the subject had undergone 20 minutes of warm-up exercise prior to the experiment, resulting in a high sweat secretion rate during the initial phase. This reduced the reabsorption of electrolytes in sweat, leading to a continuous rise in pH. After 8 minutes, sweat secretion stabilized, and the pH entered a brief plateau. By the 16-minute mark, the decrease in pH may be attributed to increased secretion of acidic metabolites such as lactic acid. After 28 minutes, as sweating intensified again, the pH showed a renewed upward trend. It is worth noting that the subject reported feeling thirsty at the 20-minute mark, accompanied by mild symptoms of dehydration, indicating a shift in the body's fluid balance status.

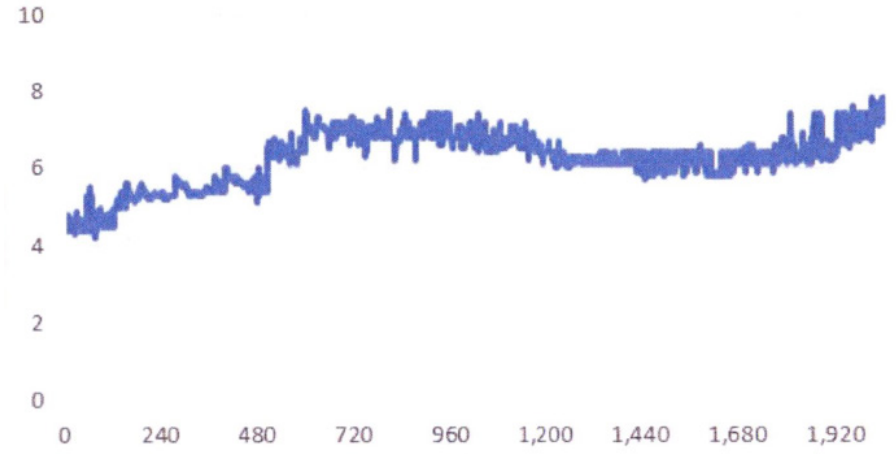

Fig. 3 Variation of Sweat pH Value Over Time During Exercise

The skin temperature data was plotted as a line chart, shown in Fig.4. It can be observed that the skin temperature rose rapidly in the initial stage and began to stabilize after approximately two minutes. Notably, the skin temperature started to increase sharply during the period when the sweat pH was rising rapidly. This phenomenon can be attributed to the substantial heat generated during physical exercise. As the skin serves as the primary organ for heat dissipation, increased blood flow to the skin during exercise enhances heat loss, thereby raising skin temperature.

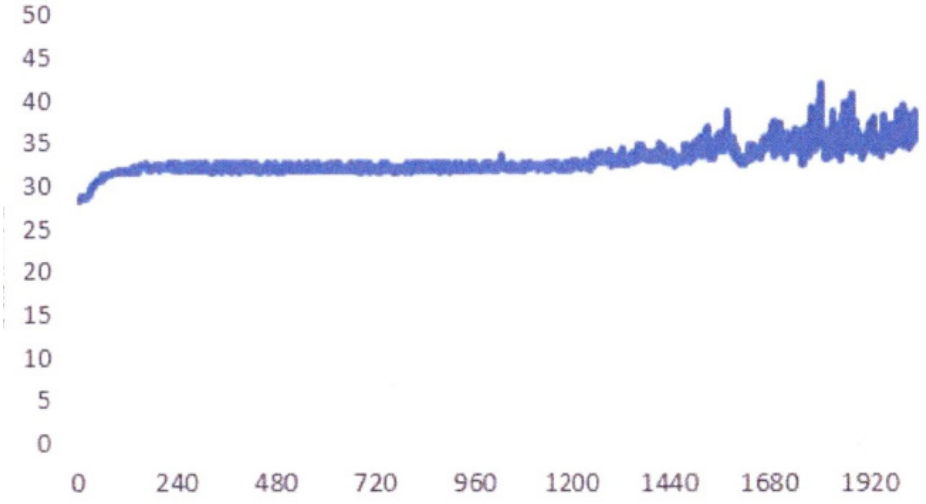

Fig. 4 Variation of Skin Temperature Over Time During Exercise

The primary value of this study lies in the integration of a pH sensor into a wearable design for sweat pH monitor-

ing, along with the development of a complete system that enables mobile data visualization. Practical experimental data have confirmed its validity, making this work a significant step toward the real-world application of sweat sensors.

3.2 Real-Time Sensing Characteristics of Flexible Sweat Sensors Based on Microfluidic Systems

The research content of this study includes the following three aspects:

(1) Based on the microchannel burst pressure theory, the relationship between burst pressure and channel width w and divergence angle β was analyzed. Experiments were conducted to determine the minimum burst pressure difference ΔPp between adjacent burst valves required for sequential sampling. Based on this, a microchannel system was designed. Finite element simulation software was used to simulate the deformation of the system under different strains, as well as the pressure and volume fraction changes of fluid passing through the burst valves. Finally, the flexible microchannels were fabricated using a replica molding method, and the sequential sampling function and the stability of the system under mechanical disturbances were experimentally verified.

(2) Based on the capillary pressure theory of micropumps, the relationship between capillary pressure and the main channel width w1 and micropillar spacing w2 was analyzed. Micropumps with different dimensions were fabricated, and experimental studies were conducted to investigate the effects of structural dimensions and initial injection rates on liquid filling time. Laser-induced graphene technology was used to fabricate and modify electrodes on PI films, enabling the preparation of glucose and sodium ion sensors, followed by performance testing. The micropumps and sensors were integrated into a flexible microfluidic device to achieve real-time quantitative measurement of analytes, and the role of the micropump in solution separation and real-time detection was explored.

(3) Integrating the previous two parts, a flexible microfluidic structure combining capillary micropumps and capillary burst valves was designed. Experiments were conducted to verify its unique filling behavior, which prioritizes filling the electrochemical region before the colorimetric region. Performance testing of both colorimetric and electrochemical sensors was carried out. The sensors were integrated into a microfluidic network to fabricate a flexible sweat sensor based on a microfluidic system. The study validated the role of capillary micropumps in promoting real-time analyte detection and the effectiveness of the colorimetric sensing region, which incorporates capillary burst valves, in detecting analytes in a time-sequential manner.

Performance Metrics:

Solutions with sodium ion concentrations of 20 mM, 40 mM, 60 mM, 80 mM, and 100 mM were injected into the microfluidic device, and the relationship between concentration and open-circuit voltage was obtained, as shown in Fig.5(a). As illustrated, the open-circuit voltage increased from 14.53 mV to 46.53 mV with rising sodium ion concentration, and the voltage signal remained relatively stable within each concentration interval. The linearity of the sodium ion sensor is shown in Fig. 5(b), where the small squares represent the average open-circuit voltage values measured at each concentration, and the dashed line denotes the fitted curve. Based on Fig.5(b), the calculated linearity reached 99.88%.

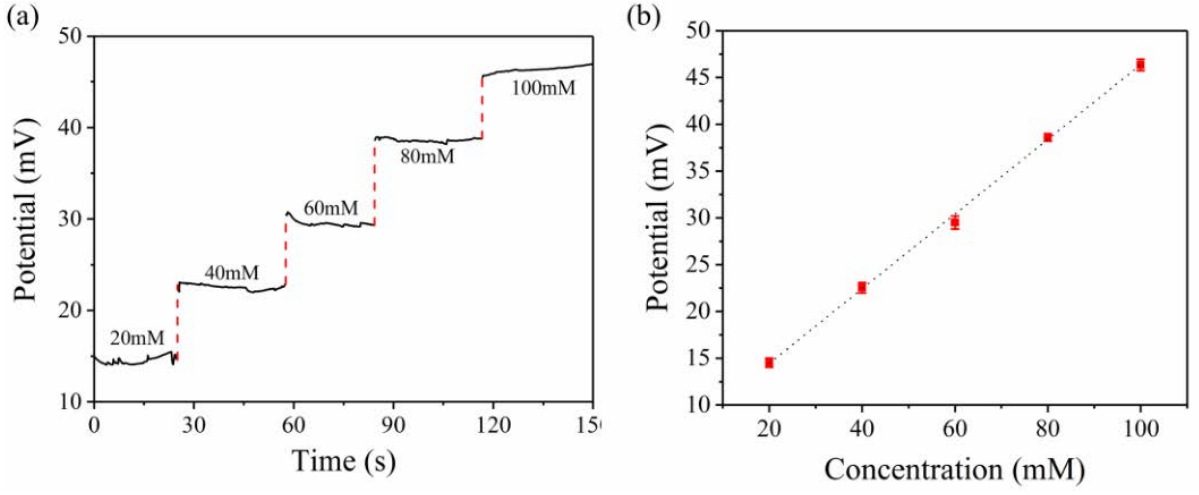

Fig. 5 (a) Na+ sensor detection ladder diagram (b) Linearity of Na+ sensor

Solutions with glucose concentrations of 4 mM, 8 mM, 12 mM, 16 mM, and 20 mM were injected into the micro-

ISSN 2959-409X

fluidic device, and the relationship between concentration and current is shown in Fig.6(a). As illustrated, the detected current increased from 12.09 μA to 50.94 μA with rising glucose concentration, while the current signal remained stable within each concentration interval without significant fluctuations. The linearity of the glucose sensor is depicted in Fig.6b, where the small squares represent the average current values measured at each concentration, and the dashed line indicates the fitted curve. Based on Fig.6(b), the calculated linearity was determined to be 99.41%.

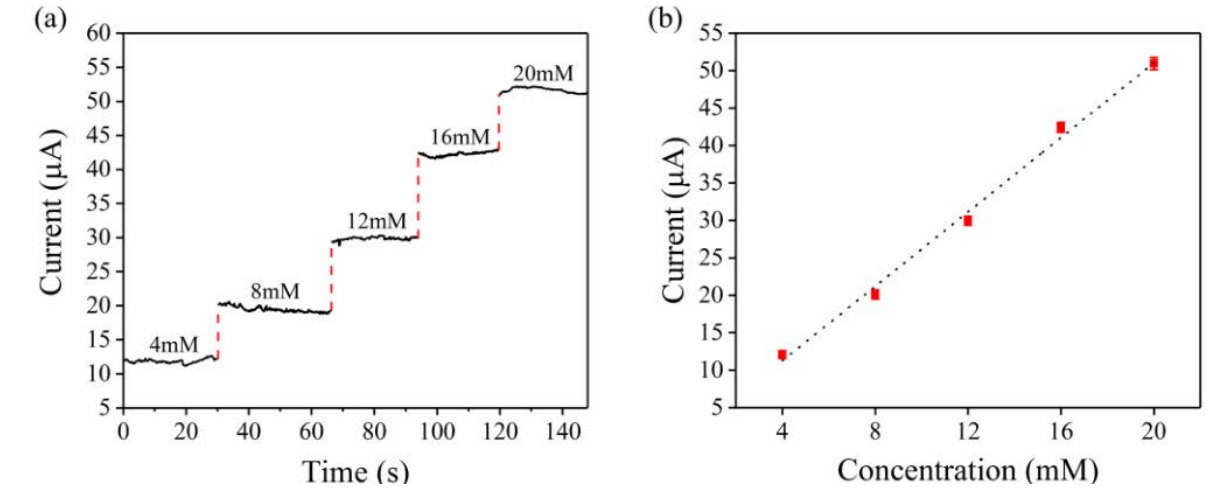

Fig. 6 (a) Glucose sensor detection ladder diagram (b) Linearity of glucose sensor

This study achieved highly accurate sodium ion and glucose detection; however, it was not adapted for practical sweat testing in wearable devices. Furthermore, due to limitations in fabrication precision, it was not possible to further reduce the range of the minimum burst pressure difference. Regarding electrochemical detection, the study utilized an electrochemical workstation to measure electrochemical signals. Nevertheless, the use of such equipment is impractical for wearable applications. The development of miniaturized flexible electronic boards is still required to enable the reception and transmission of electrochemical signals in real-world wearable settings.

3.3 Solid-State Ion-Selective Analysis for Wearable Sweat Monitoring

This study focuses on enhancing the performance and applicability of ion-selective electrodes. To improve sensor performance, materials based on redox capacitance mechanisms and electric double-layer capacitance mechanisms were explored. Furthermore, to enable better conformity to skin deformation, ion-selective electrodes capable of maintaining performance under stretching conditions were developed. The specific research efforts include:

1. A rapid and high-yield method was proposed to prepare hydrophobic and highly conductive gold nanocluster materials. When used as an intermediate layer, the resulting potassium ion electrode exhibited excellent stability, reproducibility, and strong anti-interference performance.

2. Using microfluidic technology, gold–tetrathiafulvalene hybrid materials with different morphologies were synthesized. The optimal structure was selected as the intermediate layer to develop a universal paper-based potassium ion electrode. This electrode demonstrated stable performance with almost no detectable water layer interference, making it suitable for reliable detection of potassium ions in sweat. This approach offers a new pathway for developing low-cost miniaturized sensors.

3. Carbon nanotubes were incorporated into porous carbon materials to design a necklace-like hybrid material as an intermediate layer. The calcium ion electrode constructed with this material exhibited high capacitance, fast response, low detection limit, and good reproducibility. It was successfully applied to the detection of milk and mineral water samples.

4. A highly stretchable fiber-type ion-selective electrode was designed. By coating a stretchable gold fiber with an ion-sensitive membrane and incorporating a serpentine structure, high elasticity and strong adhesion were achieved, allowing the electrode to withstand repeated and significant stretching. The design integrated sodium, chloride, and pH sensors into a headband, enabling real-time and reliable monitoring of sweat biomarkers.

To evaluate the performance of the potassium ion-selective electrode, the potentiometric response was measured in KCl solutions with concentrations ranging from 10^{-1} to 10^{-7} M. All solutions were prepared by stepwise dilution of a 0.1 M KCl stock solution. Fig.7(A) shows the dynamic response curve of the nanocluster-based potassium

ion-selective electrode. The electrode exhibited a rapid response and excellent potential stability in high-concentration KCl solutions, with only minor fluctuations observed near the detection limit in low-concentration regions. The corresponding calibration curve Fig.7(B) indicates a sensitivity of 55.1±1.22 mV/decade, a linear response range from 10^{-1} to 10^{-6} M, and a lower detection limit of 1.55×10^{-7} M. For comparison, the potentiometric response of a coated electrode was tested under the same conditions Fig.7(C-D). The results demonstrate that the nanocluster-based electrode significantly outperforms the conventional coated electrode, indicating that the use of a nanocluster membrane as a solid-state transduction layer effectively enhances the response characteristics of ion-selective electrodes.

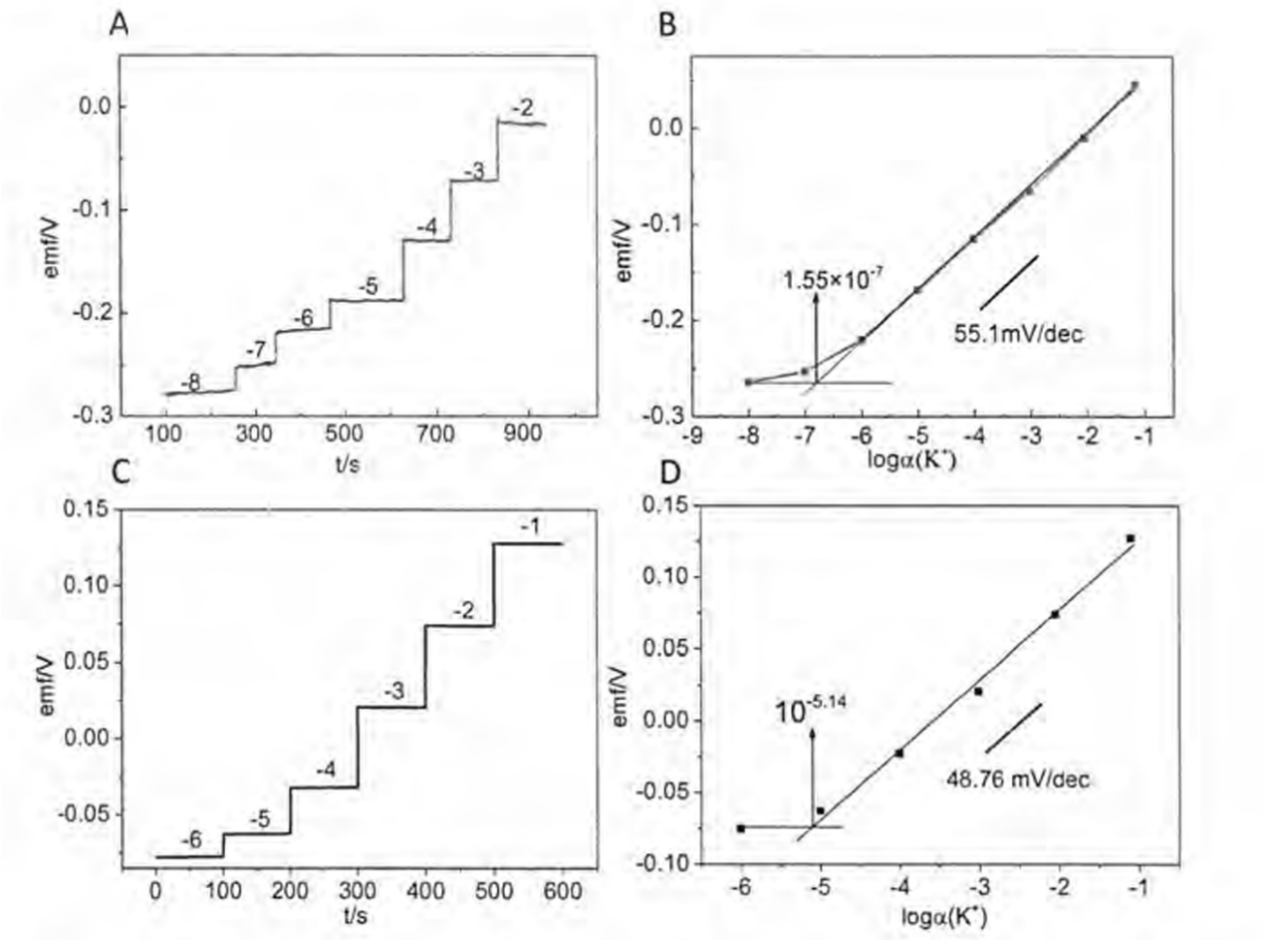

Fig. 7 (A)Time response of K^+-MPCs-ISE. (B)emf dependence on the logarithm of the activity of K+for K+MPCs-ISE. (C)Time response of K^+-ISE. (D)emf dependence on the logarithm of the activity of $K^+$for K^+-ISE.

To evaluate the practical performance of the fabricated paper-based potassium ion-selective electrode, it was applied to detect potassium ion concentrations in human sweat. Three healthy female volunteers aged 23-28 years performed steady-state exercise on an indoor elliptical trainer. After 20 minutes, sweat samples were collected from their foreheads into 1.5 mL centrifuge tubes and subsequently analyzed using the paper-based electrode coupled with an electrochemical workstation. The results are summarized in Table 1.

The potassium ion concentrations measured by the electrode fell within the range of 5.8-8.5 mM. Compared with the results obtained via inductively coupled plasma mass spectrometry (ICP-MS), the consistency between the two methods ranged from 96% to 105%, demonstrating that the developed paper-based potassium ion-selective electrode exhibits high reliability and strong potential for practical applications.

ISSN 2959-409X

Table 1. Application of the proposed method to determination of sweat samples of three healthy female(23-28 years old)and compared with the resultsof inductivelycoupled plasma roSS spectrometry(ICP-MS).

Volunteers	Concentration of potassium using ISE(mM)	Concentration of potassium using ICP-MS(mM)	Recovery(%)
1	6.4	6.7	96
2	8.5	8.1	105
3	5.8	5.9	98

The fabricated calcium ion-selective electrode (MWCNT/NPC–Ca^{2+}-ISE) showed excellent performance, with a fast response time of 2-3 seconds and high stability, making it suitable for real-time detection. It exhibited a linear response from 10^{-1} to 10^{-7} M, with a detection limit of 1.49 nM, outperforming conventional and similar composite electrodes. The sub-Nernstian response observed may be due to the low experimental temperature (16°C), and deviations at high concentrations are likely caused by the Donnan effect.

The fabricated fiber sensor was electrically connected to wires using silver paste and encapsulated with silicone rubber (Model RTV 3145) for protection. The electrode was then secured onto the surface of a headband via stitching. A healthy young female volunteer (28 years old, 48 kg) wore the sensor-integrated headband and performed steady-state exercise on a treadmill under controlled environmental conditions (20°C, 20% relative humidity). The potential signals generated during the experiment were recorded in real time using LabVIEW software. The developed wearable multi-channel paper-based sensor demonstrated the capability to simultaneously monitor changes in sodium ion concentration, chloride ion concentration, and pH value in sweat.

Simultaneously, sweat samples collected during exercise were stored in centrifuge tubes and divided into two aliquots: one was analyzed using the ion-selective electrodes integrated into the wearable device in conjunction with an electrochemical workstation, while the other was subjected to compositional analysis via inductively coupled plasma mass spectrometry (ICP-MS). pH values were measured separately using a professional pH meter. All experimental data were processed and analyzed using Origin 8.5 software, as shown in Fig.8.

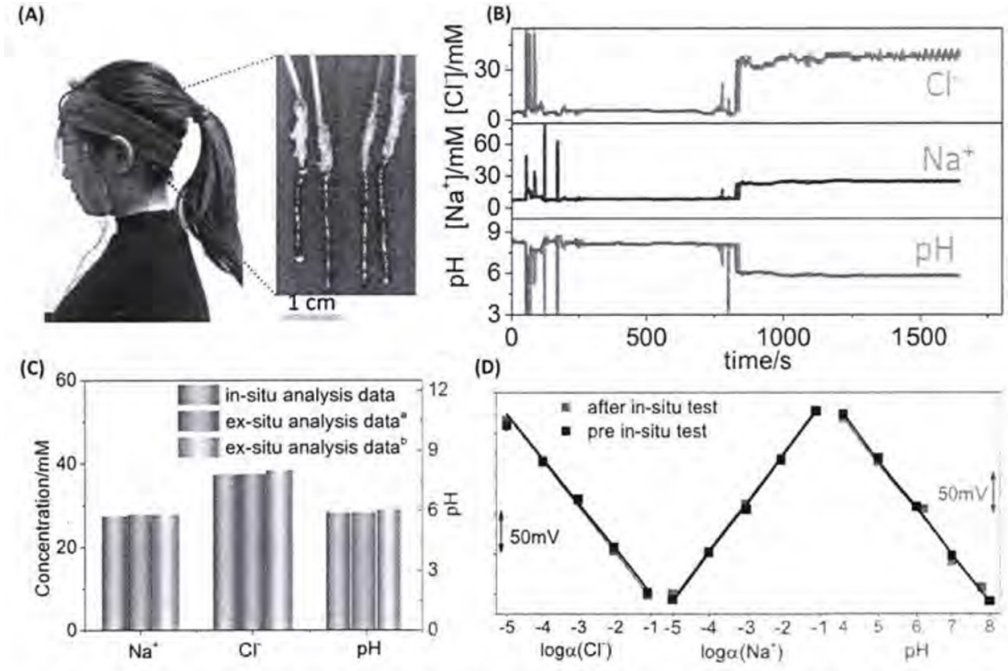

Fig. 8 Application of the integrated fiber sensors in analysis of human sweat. (A) A subject running on a treadmill while wearing the fiber sensors for sweat monitoring. (B) Real-time sweat analysis using the fiber sensors. (C) Comparison between real-time sensor data and ex situ analysis of collected sweat. (D) Calibration of Cl^-, Na^+, and pH sensors before and after on-body measurements.

This study developed a highly stretchable gold fiber-based ion-selective electrode and reference electrode. The fiber electrodes exhibited high stability, short response time, excellent selectivity, and remarkable reproducibility. When integrated into a real-time monitoring system, the test results showed strong agreement with those obtained from in vitro measurements, indicating the device's suitability for short-term monitoring of electrolyte dynamics in sweat during exercise. Additionally, the electrode can be easily assembled onto other textiles and readily adapted for detecting various target analytes by replacing the sensing unit.

However, the long-term stability of the electrode remains suboptimal, primarily due to the poor hydrophobicity and low capacitance of the gold film. Furthermore, the data acquisition chip used in this study is still relatively large, which compromises portability.

4. Discussion: The Lag in Technology Translation – Investigating Barriers to Commercialization of Early Prototypes

4.1 Early-Stage Validation of Technical Feasibility

As early as 2017 to 2020, sensing technologies in this field had already achieved relatively high precision, accompanied by advancements in system design. Research on a Real-Time Detection System for Wearable Sweat Composition demonstrated a system architecture utilizing commercial modules[1], while Solid-State Ion-Selective Analysis for Wearable Sweat Monitoring presented a high-precision wearable monitoring module [2]. Together, these studies confirmed that developing a functional sweat sensor was technically feasible.

4.2 Analysis of Technological Stagnation from an Industrialization Perspective

These two efforts occupied a transitional space between technological maturity and emergence: while academically validated, their high manufacturing costs, complex processes, and lack of reliable supply chains deterred commercial investment and hindered market entry.

The fiber-based approach in Solid-State Ion-Selective Analysis for Wearable Sweat Monitoring delivered excellent performance, but its reliance on precious metal materials and intricate fabrication methods resulted in prohibitively high costs, limiting its commercial viability [2].

Although Research on a Real-Time Detection System for Wearable Sweat Composition offered lower costs, its performance and user experience were comparatively inferior [1]. Conversely, while the high accuracy of Solid-State Ion-Selective Analysis for Wearable Sweat Monitoring was notable, it lacked corresponding integration and power solutions. The engineering development from high-performance sensors to cost-effective, reliable systems remained insufficient [2].

4.3 Supplementary Case: Challenges in Translating Research into Practical Applications

The challenges discussed in this paper are by no means isolated cases. For instance, the 2020 study Real-Time Sensing Characteristics of a Flexible Sweat Sensor Based on Microfluidic Systems demonstrated a novel sensor utilizing nanomembranes, which exhibited improved sensitivity compared to conventional approaches [3].

However, this research focused primarily on material-level modifications and relied on expensive instruments for testing under laboratory conditions, making it difficult to translate the findings into a practical wearable system.

This work is emblematic of a large body of research in the field: while many studies enhance sensor accuracy or refine certain design aspects, they often fall short of contributing to a fully functional wearable system. This further underscores that significant additional effort is required to bridge the gap between academic innovation and market-ready products.

4.4 Summary: The Divide between Laboratory and Market

In summary, these two early studies reveal that between the laboratory validation of a concept and its eventual transformation into a commercial product lies a significant gap—one shaped by cost, supply chain constraints, engineering feasibility, and market demand. Many advanced technologies may have emerged years ago, yet still struggle to cross this divide.

5. Conclusion

This retrospective analysis of two early publications demonstrates that the fundamental technological pathways for wearable sweat sensing had already been established years ago. However, the development of the technology has not progressed toward maturity and practical application as rapidly as anticipated.

Based on the above analysis, future research in wearable sweat sensing should place greater emphasis on aligning technological approaches with real-world application needs. It is advisable to prioritize the development of highly reliable devices based on mature and low-cost

ISSN 2959-409X

processes, focusing on optimizing and integrating existing technologies rather than solely pursuing performance limits. Additionally, interdisciplinary collaboration should be strengthened to construct systemic solutions that balance accuracy, stability, and wearability. Furthermore, establishing evaluation frameworks that better reflect real-world usage scenarios is recommended to facilitate the transition of research outcomes from the laboratory to industrial applications, ultimately enabling the large-scale adoption of wearable sweat sensing technology in health monitoring.

References

[1] Wu Qingcai. Research on a real-time detection system for wearable sweat composition [Master's thesis]. Beijing: University of Chinese Academy of Sciences, 2017.

[2] Xu Jianan. Solid-state ion-selective analysis for wearable sweat monitoring [PhD dissertation]. Changchun: Changchun Institute of Applied Chemistry, Chinese Academy of Sciences, 2020.

[3] Yu Shuhui. Real-time sensing characteristics of flexible sweat sensors based on microfluidic systems [Master's thesis]. Hangzhou: Zhejiang University of Technology, 2020.

[4] Mena-Bravo A, Luque de Castro M D. Sweat: a sample with limited present applications and promising future in metabolomics. Journal of Pharmaceutical & Biomedical Analysis, 2014, 90(1): 139–147.

[5] Sato K, Kang W H, Saga K, Sato K T. Biology of sweat glands and their disorders. II. Normal sweat gland function. Journal of the American Academy of Dermatology, 1989, 20: 537–563.

[6] Raiszadeh M M, Ross M M, Russo P S, Schaepper M A, Zhou W, Deng J, Ng D, Dickson A, Dickson C, Strom M, Osorio C, Soeprono T, Wulfkuhle J D, Petricoin E F, Liotta L A, Kirsch W M. Proteomic analysis of eccrine sweat: implications for the discovery of schizophrenia biomarker proteins. Journal of Proteome Research, 2012, 11(4): 2127–2139.

[7] Barrio Gómez de Agüero M I, García Hernández G, Gartner S, Grupo de Trabajo de Fibrosis Quística. Protocol for the diagnosis and follow-up of patients with cystic fibrosis. Anales de Pediatría, 2009, 71(3): 250–264.

[8] Zhang Qihua, Cheng Xuesong. Cystic fibrosis. International Journal of Nursing Sciences, 2009, 28(4).

[9] de la Torre R, Pichini S. Usefulness of sweat testing for the detection of cannabis smoke. Clinical Chemistry, 2004, 50(11): 1961–1962.

[10] Taylor J R, Watson I D, Tames F J, Lowe D. Detection of drug use in a methadone maintenance clinic: sweat patches versus urine testing. Addiction, 1998, 93: 847–853.

[11] Sears M E, Kerr K J, Bray R I. Arsenic, cadmium, lead, and mercury in sweat: a systematic review. Journal of Environmental and Public Health, 2012: 184745.

[12] Kamei T, Tsuda T, Mibu Y, Kitagawa S, Wada H, Naito K, Nakashima K. Novel instrumentation for determination of ethanol concentrations in human perspiration by gas chromatography and the interrelationship between ethanol concentrations in sweat and blood. Analytica Chimica Acta, 1998, 365(1): 259–266.

[13] Schmid-Wendtner M H, Korting H C. The pH of the skin surface and its impact on the barrier function. Skin Pharmacology and Physiology, 2006, 19(6): 296–302.

[14] Patterson C, Cornell C, Carbone B, et al. Protein depletion and metabolic stress in elderly patients with hip fractures. Journal of Orthopaedic Trauma, 1992, 6(4).

[15] Reddy M M, Wang X F, Quinton P M. Effect of cytosolic pH on epithelial Na+ channel in normal and cystic fibrosis sweat ducts. The Journal of Membrane Biology, 2008, 225(1): 1–11.